Supporting Information for:

An Autodecomposition Approach for the Low-Temperature Mesostructuring of Nanocrystal Semiconductor Electrodes.

Néstor Guijarro, Mathieu S. Prévot, Xavier Jeanbourquin, Xiaoyun Yu and Kevin Sivula*.

Laboratory for Molecular Engineering of Optoelectronic Nanomaterials, Institute of Chemical Sciences and Engineering, École Polytechnique Fédérale de Lausanne (EPFL), Station 6, 1015-Lausanne, Switzerland.

*kevin.sivula@epfl.ch

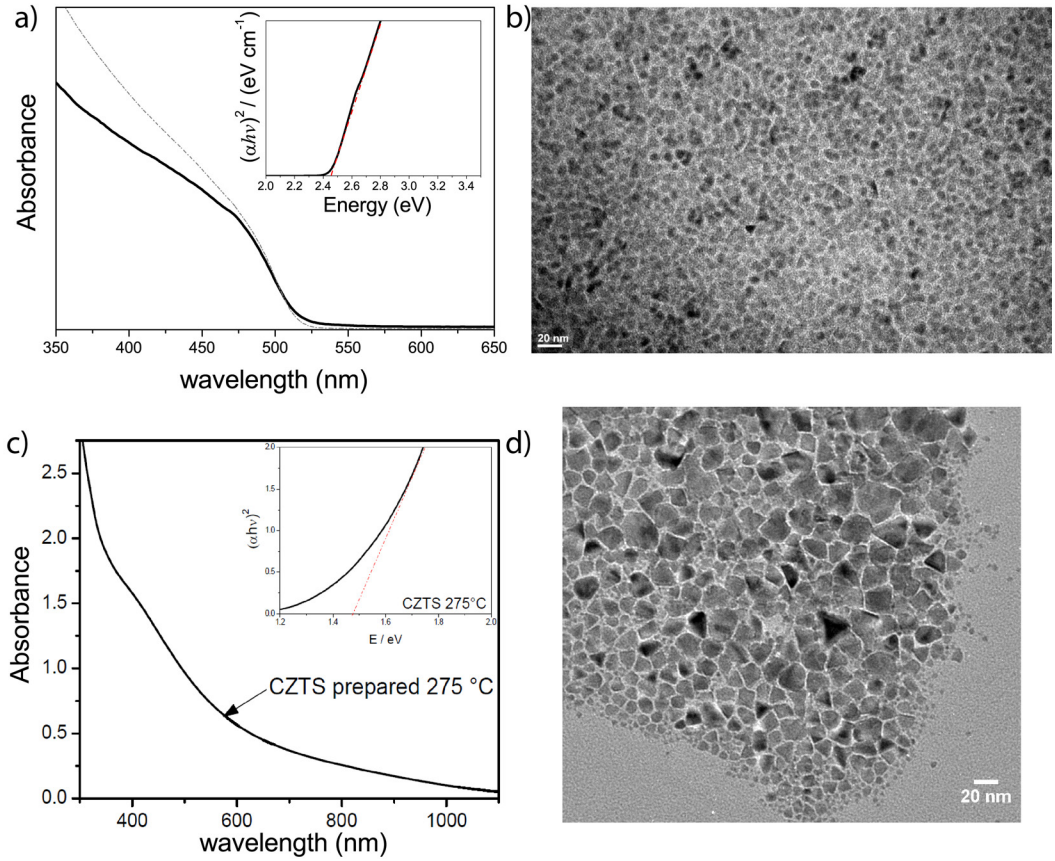

Figure S1. Characterization of the chalcogenide nanocrystals used in this work. (a) UV-VIS absorption spectrum for CdS colloidal nanocrystals dispersed in chloroform (dashed line) and for a mesoporous CdS thin film (solid line); inset diagram showing the Tauc plot for determination of the band gap. (b) TEM image of CdS colloidal nanocrystals. (c) Absorption spectrum of CZTS colloidal dispersion in chloroform and the corresponding Tauc plot (inset), (d) the corresponding TEM image of CZTS colloidal nanocrystals.

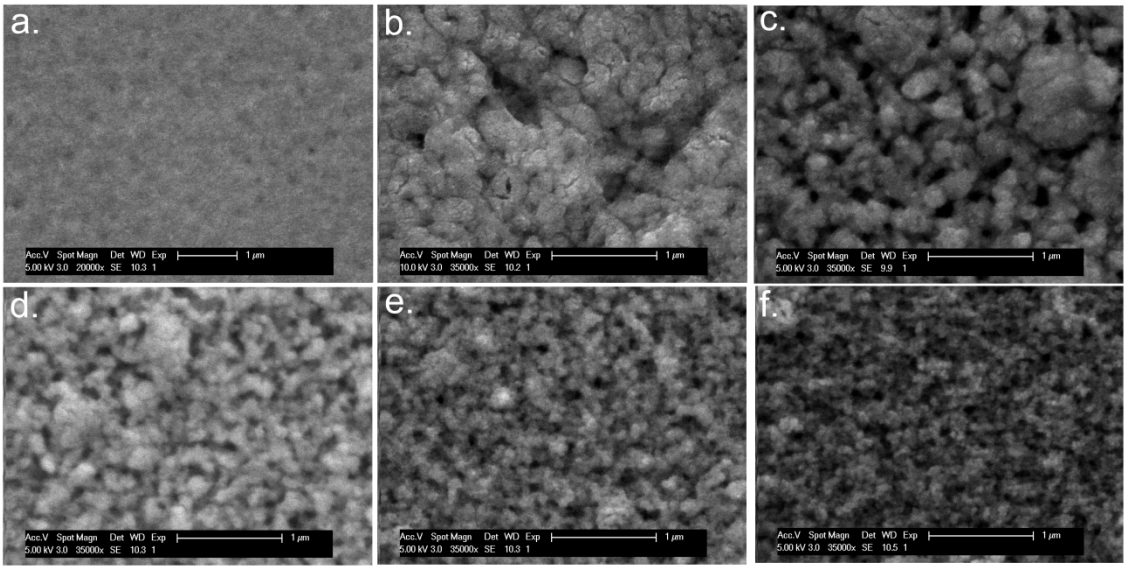

Figure S2. Top view SEM images for annealed CZTS thin films prepared with ink solutions containing nitrocellulose mass loadings of (a) 0 wt%, (b) 3.8 wt%,(c) 5.7 wt%,(d) 7.4 wt%,(e) 10.7 wt% and (f) 12.3 wt%.

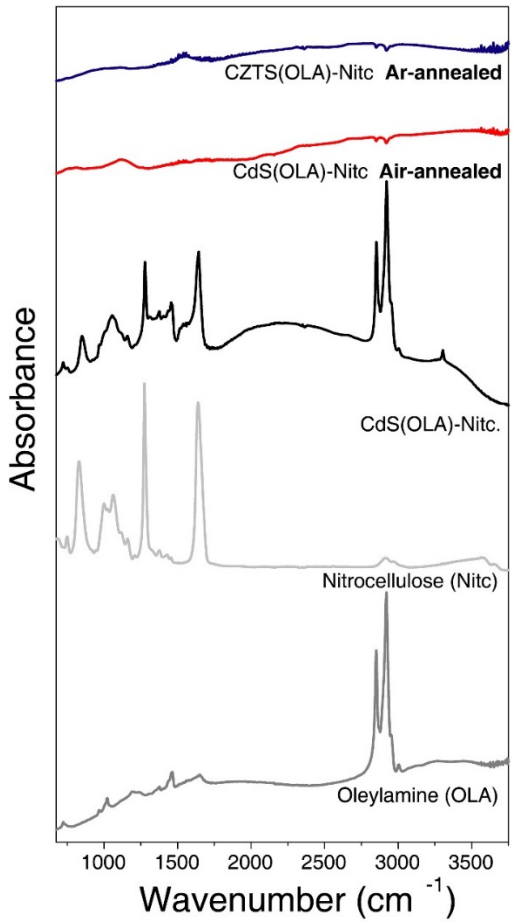

Figure S3. FT-IR spectra of CdS and CZTS nanocrystal thin film (nitrocellulose loading of 12.3 wt%) before and after annealing at 300°C for one hour. The FTIR spectra of oleylamine and nitrocellulose are also shown for reference.

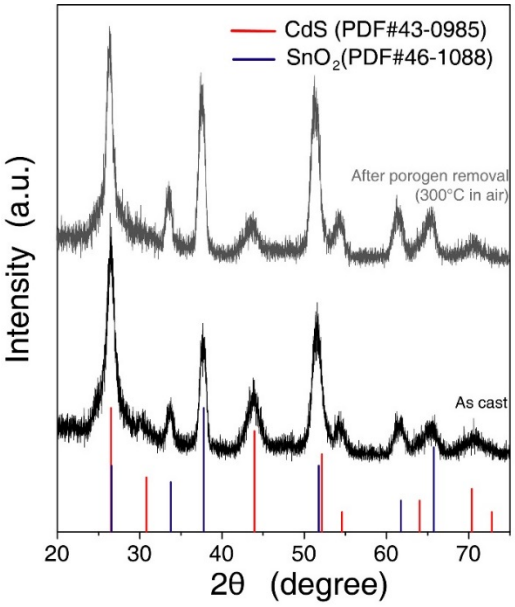

Figure S4. XRD diffraction patterns for the 12.3 wt% nitrocellulose thin film as cast and after annealing in air at 300°C for 1 hour.

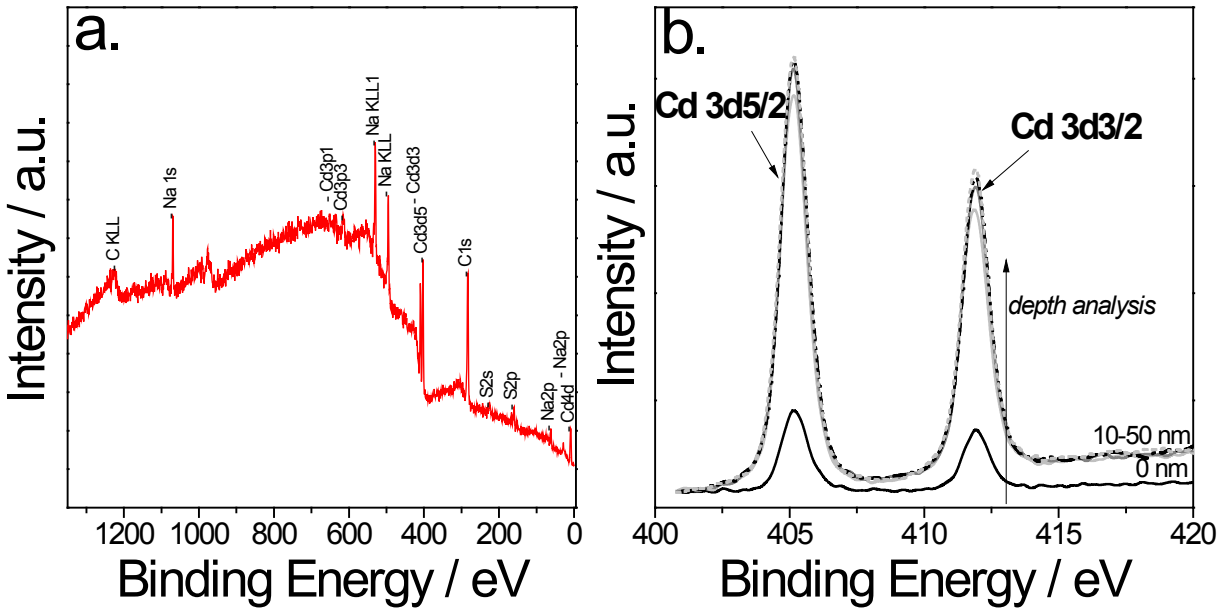

Figure S5. (a) XPS survey spectrum for the 12.3 wt% nitrocellulose CdS mesoporous thin film. (b) Spectra for the Cd 3d lines as a function of the depth (0, 10, 20, 30, 40 and 50 nm). The survey reveals the peaks associated with Cd and S, as well as peaks of Na likely coming from the electrolyte used for PEC measurements. Note that the peaks associated to C are only present on the surface of the film which indicates that originates from surface contamination rather than being the residue of the nitrocellulose decomposition. Likewise, no peaks associated with N were detected, which suggest the complete removal of the porogen in agreement with the FT-IR measurements (Figure S3). The Cd 3d5/2 appears centered at around 405.15 eV, without significant deviation when probing in depth (0 to 50 nm). This value matches quite well with the signal associated to Cd 3d5/2 in CdS which is reported to be 405.3 eV, and rules out the presence of CdO which would display a smaller value (404.6 eV).

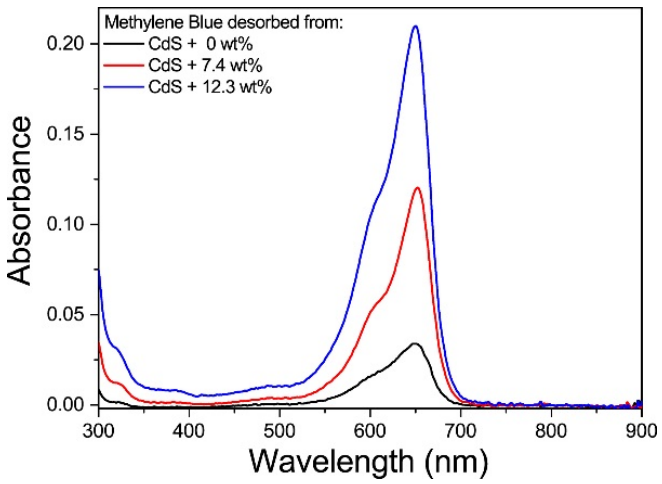

Figure S6. Absorption spectra of solutions containing desorbed methylene blue from CdS films with and without nitrocellulose.

Table S1. Relative change of the specific surface area and of the current density for CdS electrodes.

Sample	Relative Specific Surface Area[a] (Abs/Abs$_{flat}$ at 650 nm)	Relative current density[a] (j/j_{flat} at -0.5 V vs. Ag/AgCl)
CdS + 0 wt%	1	1
CdS + 7.4 wt%	3.56	4.77
CdS + 12.3 wt%	6.21	8.29

[a] Reported values correspond to the average over three different films for each sample.

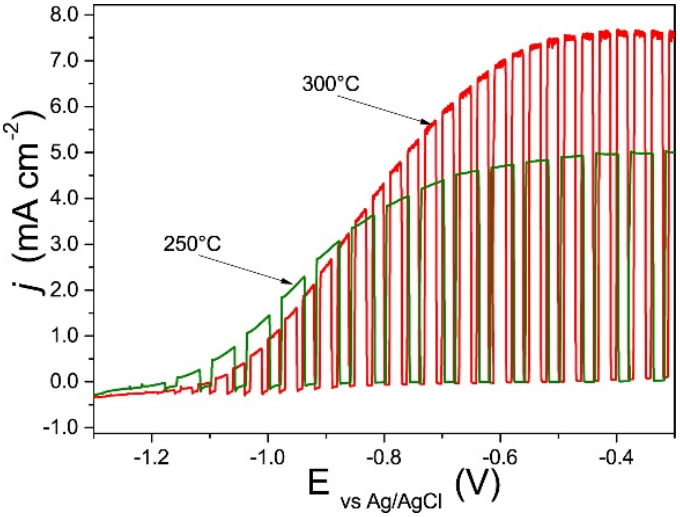

Figure S7. CdS + 12.3 wt% Nitrocellulose annealed at 250°C compared to the 300°C case.

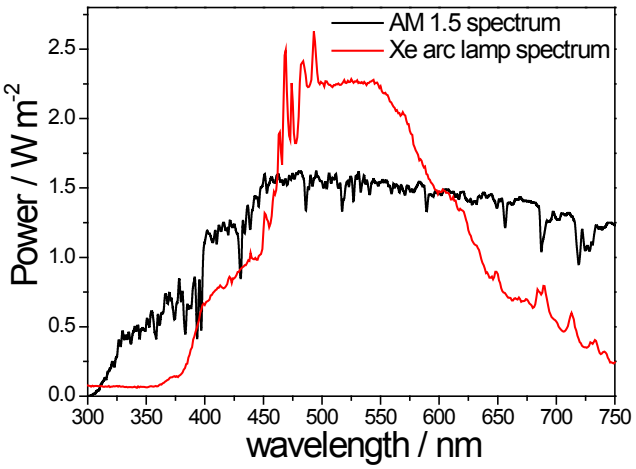

Figure S8. Xe arc lamp spectrum coupled with a UV cut-off filter and calibrated with the solar AM 1.5 spectrum to deliver the same number of photons in the range between 300 nm and 550 nm. Notably, the theoretical maximum photocurrent density attainable by CdS (band gap 2.4 eV) under AM1.5G, considering that all the incident photons with energies above the band gap contribute to the current, is ~7.5 $mAcm^{-2}$.

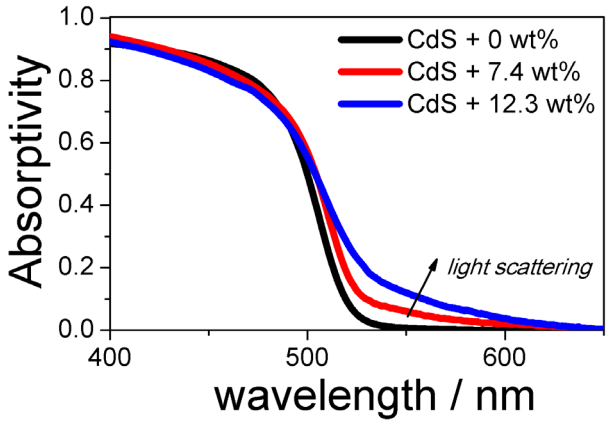

Figure S9. Absorption spectra of the ca. 200 nm CdS films. We note that a small increase in absorbance is measured with increasing nitrocellulose loading due to light scattering, as indicated by the increasing strength of the sub-bandgap scattering tail.